ORIGINAL RESEARCH

Successful in vivo hyperthermal therapy toward breast cancer by Chinese medicine shikonin-loaded thermosensitive micelle

Yonghua Su[1,]*
Nian Huang[1,]*
Di Chen[2,]*
Li Zhang[2,]*
Xia Dong[2]
Yun Sun[2]
Xiandi Zhu[2]
Fulei Zhang[2]
Jie Gao[2]
Ying Wang[2]
Kexing Fan[2]
Puichi Lo[3]
Wei Li[2]
Changquan Ling[1]

[1]Department of Integrative Oncology, Changhai Hospital of Traditional Chinese Medicine, [2]International Joint Cancer Institute, The Second Military Medical University, Shanghai, [3]Department of Biomedical Sciences, City University of Hong Kong, Kowloon Tong, Hong Kong, China

*These authors contributed equally to this work

Correspondence: Changquan Ling
Department of Integrative Oncology, Changhai Hospital of Traditional Chinese Medicine, The Second Military Medical University, Shanghai 200433, China
Tel +86 21 8187 3143
Fax +86 21 8187 3143
Email changquanling@smmu.edu.cn

Wei Li
International Joint Cancer Institute, The Second Military Medical University, Shanghai 200433, China
Tel +86 21 8187 0804
Fax +86 21 8187 0801
Email liwei@smmu.edu.cn

Abstract: The Chinese traditional medicine Shikonin is an ideal drug due to its multiple targets to tumor cells. But in clinics, improving its aqueous solubility and tumor accumulation is still a challenge. Herein, a copolymer with tunable poly(N-isopropylacrymaide) and polylactic acid block lengths is designed, synthesized, and characterized in nuclear magnetic resonance. The corresponding thermosensitive nanomicelle (TN) with well-defined core-shell structure is then assembled in an aqueous solution. For promoting the therapeutic index, the physical-chemistry properties of TNs including narrow size, low critical micellar concentration, high serum stability, tunable volume phase transition temperature (VPTT), high drug-loading capacity, and temperature-controlled drug release are systematically investigated and regulated through the fine self-assembly. The shikonin is then entrapped in a degradable inner core resulting in a shikonin-loaded thermosensitive nanomicelle (STN) with a VPTT of ~40°C. Compared with small-molecular shikonin, the in vitro cellular internalization and cytotoxicity of STN against breast cancer cells (Michigan Cancer Foundation-7) are obviously enhanced. In addition, the therapeutic effect is further enhanced by the programmed cell death (PCD) specifically evoked by shikonin. Interestingly, both the proliferation inhibition and PCD are synergistically promoted as T > VPTT, namely the temperature-regulated passive targeting. Consequently, as intravenous injection is administered to the BALB/c nude mice bearing breast cancer, the intra-tumor accumulation of STNs is significantly increased as T > VPTT, which is regulated by the in-house developed heating device. The in vivo antitumor assays against breast cancer further confirm the synergistically enhanced therapeutic efficiency. The findings of this study indicate that STN is a potential effective nanoformulation in clinical cancer therapy.

Keywords: thermosensitive micelle, shikonin, breast cancer, intra-tumor accumulation, critical micelle concentration, hyperthermal therapy, in vivo

Introduction

Breast cancer is the most common cause of cancer mortality in women aged from 20 to 59 years, and accounts for 29% of new cancer incidence in women.[1] Despite the development of surgery, radiotherapy, targeted therapy, and systemic treatment in the past few decades, the patients with advanced breast cancer (stage IV) still often suffer from serious side effects in clinical trials.[2] The adverse prognosis is mainly attributed to nonspecific absorption of chemotherapeutic drugs in normal tissues.[3–5] Hence, different strategies have been developed for breast cancer therapy for improving the safety and efficacy. The critical issue is to seek a suitable drug that holds multi-targets to tumor and mild toxicity to normal tissue.[6,7] Shikonin, which is derived from the traditional Chinese medicine named as "Zi Cao," is the root of *Lithospermum erythrorhizon*

Sieb. Et Zucc., *Alkanna tinctoria*, *Arnebia euchroma* (Royle) Johnst, and *Arnebia guttata* Bunge.[8] Previous studies have demonstrated its significant antitumor efficacy toward breast cancer with following multifunctions: 1) shikonin can inhibit signal transducer and activator of transcription (STAT) (3), focal adhesion kinase, and Src activation and decrease the expression of breast cancer stem cell-associated markers;[9,10] 2) it can downregulate the expression of steroid sulfatase genes that relate to the biosynthesis of estrogen within breast tumors;[11] 3) it can suppress breast cancer cell invasion and migration by inhibiting epithelial mesenchymal transition (EMT)[12] and matrix metalloproteinase-9 (MMP-9);[13] and 4) it can circumvent cancer drug resistance in breast cancer cells.[14] The multi-targets of shikonin to tumor inhibition indicate that it is an excellent candidate for cancer therapy. However, the therapeutic efficacy of shikonin is somewhat limited due to poor aqueous solubility and extensive first-pass metabolism, which are similar to those of many other chemotherapeutic drugs.[15,16] Thus, designing new formulations, which can obviously increase shikonin solubility and decrease its toxicity to normal tissue, is highly desired in clinics.

Based on the enhanced permeability and retention (EPR) effect, nanomedicine shows new hope for promoting the traditional chemotherapy because it holds many advantages including increasing the solubility of hydrophobic drugs, identifying the tumor cells, and triggering the drug release in the lesion sites.[17,18] In order to improve drug-specific accumulation in tumors, various novel stimulus-sensitive polymeric micelles were designed such as the temperature,[19] pH,[20] reduction,[21] light,[22] magnetic field,[23] and ultrasound.[24] Among these newly developed functional carriers, nanomicelles are ideal candidates for the delivery of hydrophobic shikonin. Micelles are assembled from amphiphilic block copolymers with hydrophobic core and hydrophilic corona in aqueous media.[17] The hydrophobic core holds high capacity for hydrophobic anticancer drugs loading via the similar-to-similar interaction, while the hydrophilic corona can protect micelles from the reticuloendothelial system through reducing the interaction with serum proteins.[6]

On the other hand, it is reported that the temperature in tumor microenvironment is ~3°C–5°C higher than that in the non-tumor tissue,[25] which offers a new opportunity for nanocarrier's design. Nanocarriers containing thermosensitive polymer poly(N-isopropylacrylamide) (PNIPAM) are thus extensively studied due to their tunable volume phase transition temperature (VPTT). In the previous study, the in vitro cellular internalization of PNIPAM-based micelles is obviously enhanced at T > VPTT, that is, the temperature-regulated passive targeting.[19] The intracellular release of such drug-loaded nanomicelles with hydrophilic PNIPAM corona (thermosensitive nanomicelle [TN]) is also successfully regulated by the temperature in vitro.[21,22] On the contrary, the drug-loading content, release, and micellar stability are also strongly dependent on the hydrophobic core.[26] The China Food and Drug Administration-approved hydrophobic polymers, such as poly(ε-caprolactone) and polylactic acid (PLA), are widely used for making biodegradable micelles.[27] The pH-regulated degradation endows its function that controls the intracellular drug release in the lesion sites, which can enhance therapeutic efficacy.[28,29] Therefore, it is easy to find that micelles with temperature-responsive and degradable merits are a promising platform for shikonin delivery. In the further study, it was found that improving the in vivo passive targeting and cellular uptake is still a big challenge in practical application.[30]

In this study, focusing on the in vivo antitumor therapy of shikonin-loaded thermosensitive nanomicelle (STN), an STN formulation was designed and prepared. The physical chemistry properties, including the size, structure, critical micelle concentration (CMC), serum stability, VPTT, temperature-regulated passive targeting and drug release, in vitro cellular internalization, cytotoxicity, and possible apoptosis/necrosis, were systemically investigated. Subsequently, the in vivo biodistribution, temperature-regulated inhibition of subcutaneous breast tumor growth, was firstly realized by the in-house developed tumor temperature regulator. The therapeutic efficiency and detailed mechanisms of such STNs were then evaluated and clarified in vitro and in vivo.

Materials and methods
Materials
N-Isopropylacrylamide (NIPAM) was obtained from Kojin (Tokyo, Japan) and purified by recrystallization from n-hexane. N,N-dimethylacrylamide (DMAAm) (Wako Pure Chemical Industries, Ltd., Osaka, Japan) was distilled under reduced pressure. D,L-Lactide (LA) (Tokyo Chemical Industry, Tokyo, Japan) was recrystallized from ethyl acetate. e-Caprolactone, N,N-dimethylformamide, 2,20-azobis (2-methyl-N-[hydroxyethyl]) propionamide (VA-086), dimethyl sulfoxide, tetrahydrofuran (THF), N,N-dimethylacetamide (DMAC), xylene, diethyl ether, sodium thiosulfate ($Na_2S_2O_4$), disodium phosphate, monosodium phosphate, hydrodated phosphotungstate, 4% paraformaldehyde, tetramethylrhodamine-5-carbonyl azide (rhodamine, or Carboxytetramethylrhodamine), and highly purified 1,4-dioxane were provided by Wako Pure Chemical Industries, Ltd. Maleimide (Mal), tin(II) 2-ethylhexanoate,

shikonin, fluorescein isothiocyanate (FITC), and 4′,6-diamidino-2-phenylindole (DAPI) were purchased from Sigma-Aldrich Co. (St Louis, MO, USA). 2-Hydroxyethylamine and 2-ethanolamine were obtained from Kanto (Tokyo, Japan) and were used as received. Dulbecco's Modified Eagle's Medium (DMEM), fetal bovine serum (FBS), and Dulbecco's phosphate-buffer solution (PBS) were purchased from Thermo Fisher Scientific (Waltham, MA, USA). A reversible addition-fragmentation chain transfer (RAFT) agent, 2-(N-[2-hydroxyethyl]carbamoyl) prop-2-yl dithiobenzoate (HECPD), was prepared according to previous publications.[28,31–33] The water used was purified by a Milli-Q water purification system (EMD Millipore, Billerica, MA, USA). The dialysis membrane was provided by Spectrum Medical Industries (Los Angeles, CA, USA).

Cell lines and nude mice

The cell lines of human embryonic kidney (293T) and breast cancer (Michigan Cancer Foundation [MCF]-7) were purchased from American Type Culture Collection (ATCC) (Manassas, VA, USA). Both were cultured in the following medium: DMEM supplied with 10% FBS, 50 units/mL penicillin, and 50 µg/mL streptomycin at 37°C with 5% CO_2. Before the in vitro cytotoxicity and other experiments, the cells were precultured until confluence was reached to 75%. The female BALB/c nude mice were obtained from the Animal Experimental Center of The Second Military Medical University. This study protocol was approved by the ethical review boards of The Second Military Medical University. Animal welfare and experimental procedures were carried out in accordance with the National Research Council's Guide for the use of laboratory animals.

Synthesis and characterization of the PID_{118}-b-PLA_{39} block copolymer

The PNIPAM-c-DMAAm random copolymer with 118 comonomer unit (PID_{118}-OH) was prepared by RAFT.[28] Figure 1 shows the synthesis process. A proportional amount of phenal-PID_{118}-OH (0.015 mmol), 2 mol equivalents of $Na_2S_2O_4$, and 40 mol equivalents of Mal (vs terminal groups) were dissolved in 5 mL THF pre-deoxidized by N_2 for 1 hour. 2-Ethanolamine (20 mol equivalents vs terminal dithiobenzoate groups) in 1 mL pre-deoxidized THF was slowly dropped into the polymer solution under N_2 bubbling followed by 20-hour reaction at room temperature. After reaction, the solution was dialyzed against Milli-Q water using the dialysis membrane (molecular weight cut off [MWCO] =1,000 D) until complete removal of the unreacted chemicals and the

organic solvent THF. Then the final white product polymers with Mal end group were recovered by freeze-drying.

As shown in Figure 1, the block copolymer (PID_{118}-b-PLA_{39}) was synthesized using PID_{118} as the macro-chain transfer agents. In the conventional ring-open polymerization, proportional calculated amounts of monomers were weighed, and PID_{118} (0.75 g, 6×10^{-5} mol) and LA (0.5 g, 10 mM) were mixed in a 25 mL nash flask connected with a condenser. The mixed powder was dried at 50°C under vacuum for about 2 hours. Then pre-degassed xylene (4 mL) was injected into each flask under argon. The imitator tin(II) 2-ethylhexanoate (40 mg) pre-dissolved in ~2 mL pre-degassed xylene was injected into the monomer solution under argon. The polymerization was carried out at 150°C for 24 hours. After polymerization, the solutions were distilled at 50°C under vacuum to remove xylene and redissolved in 5 mL THF. The precipitation was removed by centrifugation. The up-clear solution was collected and precipitated in excess diethyl ether two times. The pale powder was obtained under vacuum drying. The molecular weight and polydispersity index (PDI) of such thermosensitive biodegradable block copolymer were characterized by ^{1}H nuclear magnetic resonance (NMR) (400 MHz, Varian Inc., Palo Alto, CA, USA) using chloroform-d as a solvent.

Self-assembly of TNs

The micelles were prepared by the dialysis method mentioned in the previous publications.[28,29] The PID_{118}-b-PLA_{39} block copolymer (~10 mg) was dissolved in 1.5 mL DMAC and then dialyzed against Milli-Q water using the dialysis membrane (MWCO =1,000 D) at 24°C for 48 hours with regular water changing. The hydrodynamic diameter and size distribution were determined by ZetaSizer Nano-ZS (Malvern Instruments, Malvern, UK). The morphology of TN was confirmed by transmission electron microscope (TEM) (H-7000 electron microscope; Hitachi, Tokyo, Japan) at 85 kV.

CMC testing

Fluorescence spectra were recorded by an FP-6500 spectrofluorimeter (JASCO Corporation, Tokyo, Japan) using pyrene as a hydrophobic fluorescence indicator. Excitation and emission bandwidths were 10 and 3 nm, respectively. Pyrene was dissolved in acetone with a concentration of 100 µM. Then the pyrene solution (~5 µL) was dropped into 2 mL of each micelle solution with concentrations from 1×10^{-3} to 1 mg/mL. The sample solutions were then stirred at 20°C for ~2 days to remove acetone completely. The fluorescence excitation was carried out at 374 nm and the emission spectra were recorded from 350 to 450 nm.
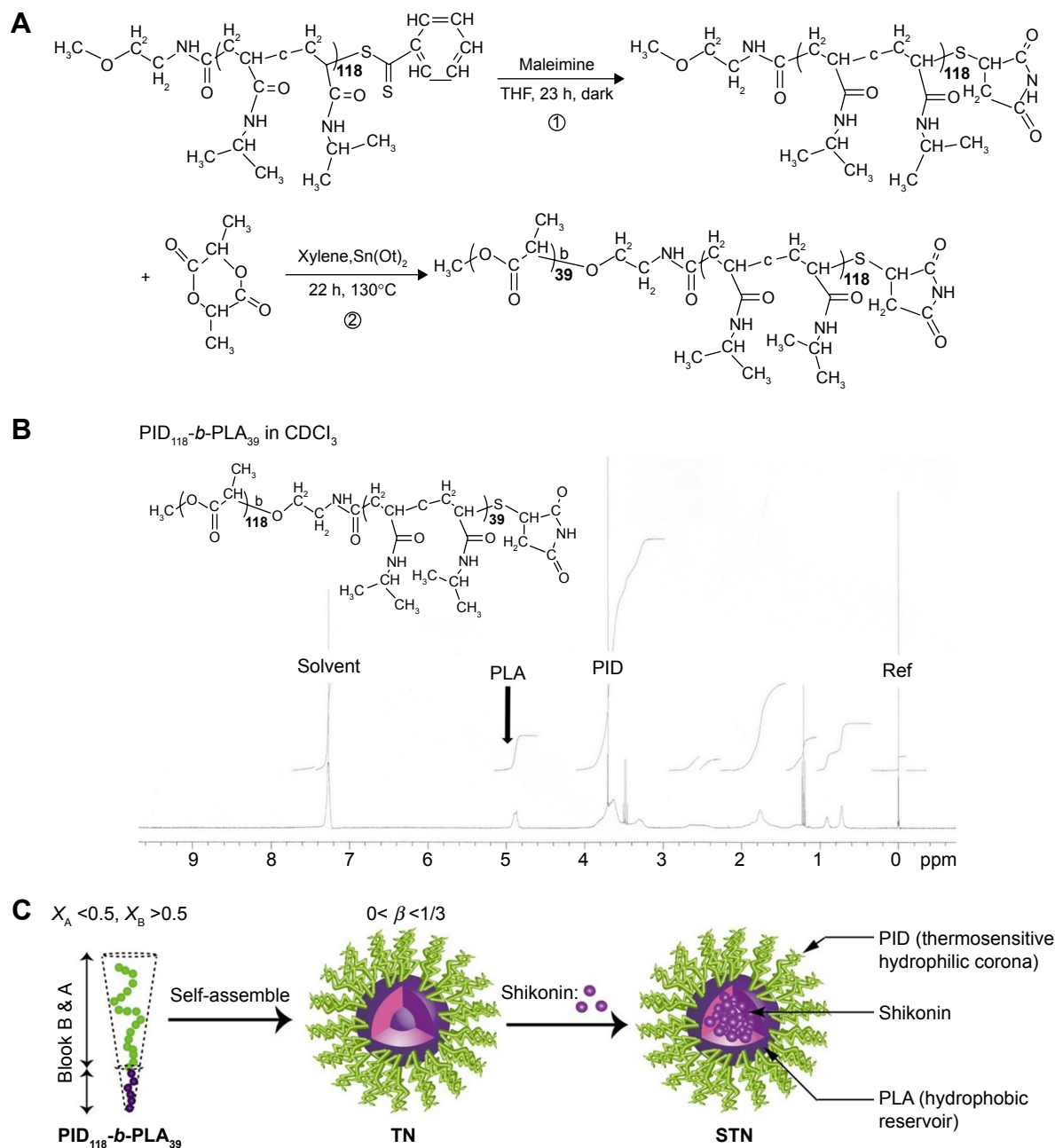
Figure 1 (**A**) Synthesis process of PID$_{118}$-PLA$_{39}$; (**B**) the NMR characterization of the copolymer in CDCl$_3$; and (**C**) the assembly process of TN.
Abbreviations: PID, PNIPAM-c-DMAAm random copolymer; PNIPAM, poly(N-isopropylacrymaide); DMAAm, N,N-dimethylacrylamide; PLA, polylactic acid; CDCl$_3$, chloroform-d; TN, thermosensitive nanomicelle; THF, tetrahydrofuran; STN, shikonin-loaded thermosensitive nanomicelle; NMR, nuclear magnetic resonance.

In the emission spectra, the first vibration band (0-0 band, I$_1$) showed a significant change but the third vibration band (I$_3$) had a little variation in response to the changes in microenvironment polarity. Thus, the intensity ratio of the first band to the third band (R=I$_1$/I$_3$) was strongly related to the polarity of the surrounding medium of the indicator pyrene. The CMC value can be obtained from I$_1$/I$_3$.[34–36]

Temperature-sensitive properties

An ultraviolet (UV)–vis spectrometer (V-530; Japan Spectroscopic Co., Ltd, Tokyo, Japan) fitted with a temperature and stirring controller was used to monitor the percentage transmittance of light at 500 nm passing through the sample cell. The micelle solution (~4 mL, concentration ~2 mg/mL) tuned by PBS (pH ~7.4) was added to an UV cell with a stirring bar and located on the cell holder. The VPTT of the micelle solution was defined at the absorption of the micellar solution sharply decreased to 50%.

Drug loading and releasing profile of STN

The PID$_{118}$-b-PLA$_{39}$ block copolymer (~12 mg) was dissolved in 12 mL DMAC. The shikonin was dissolved in

DMAC with a concentration of ~2 mg/mL. Then a tri-ethylamine (TEA) solution with 1.5 m equivalents to the shikonin in DMAC was prepared and diluted ten times by DMAC. The TEA solution was slowly dropped to the shikonin solution and kept stirring for ~5 minutes. Then the shikonin and polymer were mixed with a volume ratio of 5:5. The mixture was dialyzed against Milli-Q water after stirring for ~2 minutes. The shikonin-micelle complex was collected and stocked for further use. Its concentration and loading content were measured by UV at 516 nm and calculated by the ratio of weight of drug in micelles ($W_{drug\ in\ micelle}$) to weight of micelles ($W_{micelle}$).

A dialysis bag (Spectra/pro 6 membrane [Varian Medical Systems, Inc., Palo Alto, CA, USA], MWCO =1,000 D) containing ~6 mL of the shikonin-micelle solution was put in a beaker with 1,000 mL Milli-Q water tuned by PBS (pH =7.4). The beaker was fixed in a water bath kept at 37°C and 40°C with stirring. The initial shikonin concentration in the micelle was ~0.15 mg/mL. The shikonin-micelle mixture was continuing dialysis against with the PBS solution. The micelle solution (~0.2 mL) was sampled from the dialysis bag at specific time intervals. Subsequently, acetonitrile (0.2 mL) was added to the collected solution and analyzed by reverse high performance liquid chromatography to determine the amount of shikonin reversed in the dialysis bag.

In vitro cellular uptake

The MCF-7 cells were seeded into a 24-well microplate (2×10^5 cells/mL, 0.25 mL/well) and cultured for ~2 days till the cells reached 75% confluence. Then they were incubated with the PID_{118}-b-PLA_{39} micelle-shikonin complex solution for different times at 37°C and 40°C. Here, the high temperature was tuned by increasing the temperature of cell incubator. The MCF-7 cells were gently rinsed with DMEM/FBS twice. Then the inverse fluorescent micros-copy was used to take an image. After taking the image, the media was discarded and trypsin was used to digest the cell for ~3 minutes. Then the MCF-7 cells were rinsed with PBS and centrifuged twice at 800 rpm for 5 minutes. Finally, flow cytometry was used to check the fluorescence intensity. The in vitro cellular internalization of FITC-loaded TNs (FTNs) was investigated by confocal laser scanning microscopy (LSCM). After the culture medium was piped out and rinsed with PBS twice, the cells were fixed with 4% paraformaldehyde. The samples were visualized by TCS SP LSCM (Leica Microsystems, Wetzlar, Germany). The samples used for LSCM and flow cytometry were prepared at the same time.

In vitro cytotoxicity evaluation of TNs and STNs

For the non-cytotoxicity evaluation of TNs, the 293T cells were seeded into 96-well microplates (2×10^5 cells/mL, 100 µL/well) and cultured for 2 days. Then they were incubated with the PID_{118}-PLA_{39} micelle with concentrations of 0.01, 0.1, 0.5, and 1 mg/mL in DMEM/FBS for 24 and 48 hours at 37°C. The cells were gently rinsed with DMEM/FBS twice. The media were replaced with 100 µL of Cell Counting Kit (CCK)-8 (Dojindo, Japan), followed by 2.5-hour incubation. The absorbance was measured at 450 nm using a microplate spectrophotometer to check the cells' surviving profile. The cytotoxicity measurement of STNs against MCF-7 cells was similar to the abovementioned procedure. Here, the polymer micelles and the shikonin-micelle complex with concentration are 0.05, 0.1, 0.2, and 0.5 mg/mL (at the equivalent drug concentration: µg/mL). The absorption of the well was measured by the microplate reader with a wavelength of 450 nm. The cell viability was calculated using the following formula:

$$\text{Surviving cells (\%)} = \frac{OD_{sample} - OD_{control}}{OD_{neg} - OD_{control}} \times 100 \quad (1)$$

OD_{sample}, $OD_{control}$, and OD_{neg} are the UV absorption of the micelles, the culture medium, and the cell without micelles, respectively. The IC_{50} values were determined by constructing a dose–response curve and examining the effect of different concentrations of antagonist on reversing agonist activity. The IC_{50} values were then calculated for a given antagonist by determining the concentration needed to inhibit half of the maximum biological response of the agonist.

Annexin/propidium iodide (PI) assay

PCD was measured by the annexin V/PI assay. For the annexin-PI assay, the MCF-7 cells were incubated in 6-well transparent plates. The externalization of phosphatidylserine as a marker of early-stage apoptosis was detected by the annexin V protein conjugated to FITC, whereas membrane damage due to late-stage apoptosis/necrosis was detected by the binding of PI to nuclear DNA. After the exposure of shikonin and STN (in 37°C and 40°C, respectively), the cells were collected, washed in binding buffer, and incubated in the dark for 10 minutes at room temperature in 100 µL binding buffer containing annexin V-FITC (40 µL/mL) and PI (1 µg/mL). After incubation, the binding buffer (400 µL) was added to each sample, and the cells were kept on ice. The 488 nm laser was used for

excitation, and FITC was detected in FL-1 by a 525/30 BP filter, while PI was detected in FL-2 by a 575/30 BP filter. Standard compensation was done in the Quanta SC MPL Analysis software (Beckman Coulter; Fullerton, CA, USA) using single-stained and unstained cells. For each sample, 20,000 cells were analyzed and apoptotic (annexin V+, PI−), necrotic (annexin V+, PI+), and live (annexin V−, PI−) cells were expressed as percentages of the 20,000 cells.

In vivo distribution of FTN in nude mice bearing tumor

BALB/c nude mice aged 4 weeks were implanted with the MCF-7 cells (4×10^7 cells in PBS) in the left shoulder via subcutaneous injection. At the time point when the tumor size reached 250 mm³, the tumor-bearing mice were injected with FTN or free-FITC (5 nmol each) intravenously. After designated periods following injection, the mice were placed under isoflurane anesthesia temporarily and in vivo distributions of FTN were analyzed using the IVIS Lumina XR (PerkinElmer Inc., Waltham, MA, USA). In order to maintain the normal excretion, the mice were treated with anesthesia only during measurement. The mice were sacrificed at 24 hours after the injection, and the fluorescence images of the tumor and each organ were acquired, immediately placed in the OCT medium, and rapidly frozen in liquid nitrogen. The frozen sections were cut at 10 µm sections and fixed with acetone at −20°C. After washing with PBS, the sections were counterstained with DAPI and visualized with a fluorescence microscope.

In vivo antitumor assays of STN in nude mice

As shown in Figure 2A, the in vivo therapeutic effect of the nanomicelle was evaluated in mice bearing subcutaneous breast cancer. Briefly, 1×10^7 MCF-7 cells were injected subcutaneously into BALB/c nude mice (male, 4 weeks, ~20 g). When the tumor size had reached ~150 mm³, the mice were treated with single intravenous injections of STN (37°C), STN (40°C), free shikonin (FS), and PBS (2 mg/kg) via the tail vein. The treatment was carried out on days 0, 3, 6, 9, 12, 15, 18, 21, 24, and 27. The tumors were measured by using a caliper every 3 days, and the tumor volume was calculated by using the following formula:

$$\text{Tumor volume} = \text{Length} \times \text{Width}^2 / 2 \qquad (2)$$

where L and W were the longest and shortest diameters. Tumor progression was evaluated in terms of relative tumor volume (to day 0) over a period of 21 days. The body weight

of the mice was monitored every 3 days. The survival data were accumulated according to the death of all the mice from tumors. It should be noted that the in vivo tumor accumulation of STNs was first realized by the in-house developed heating device as shown in Figure 2B.

Statistical analysis

Data in this study were analyzed using the software SPSS 21.0 (IBM Corporation, Armonk, NY, USA). For values that were normally distributed, a direct comparison between the two groups was made by using Student's non-paired t-test. One-way analysis of variance with the Dunnett or Newman–Keuls posttest was used to compare the means of three or more groups. All the mice died from tumors. The Kaplan–Meier survival analysis was used to analyze the survival data. $P<0.05$ was considered statistically significant (*$P<0.05$; **$P<0.01$; ***$P<0.001$; and #$P>0.05$).

Results
Synthesis and characterization of TN

Figure 1A shows the preparation of PID_{118}-b-PLA_{39} block copolymer. Figure 1B shows the NMR signal of PID_{118}-b-PLA_{39}, and the characteristic signal at ~4 ppm was attributed to $-CH(CH_3)_2$ of PNIPAM and at ~3.6 ppm was assigned to $-N(CH_3)_2$ of DMAAm. The ratio of NIPAM to DMAAm in PID was about 3:1. Thus, it can be found that the characteristic peaks of PLA are at ~5.2 ppm from $-CHCH_3-$. The LA monomer unit was calculated to be ~39. Figure 1C shows the self-assembly of TN and STN in water. As shown in Figure 3, the hydrodynamic diameter and its size distribution of the PID_{118}-b-PLA_{39} micelles in aqueous solutions are narrow. The radius of the blank TN was 53 nm (Figure 3A). However, after loading the shikonin, the radius increased to 98 nm (Figure 3B). Compared with the blank micelle, the size of micelle-shikonin increased significantly because the drug molecules were entrapped inside the core. The morphology of these micelles was also characterized by TEM as shown in Figure 3C and D. The TEM picture clearly shows a well-defined core-shell structure of the corresponding micelles.

Thermosensitive property, releasing profile, CMC, cytotoxicity, and stability of TN

Figure 4A shows the temperature dependence of transmittance of PNIPAM and PID_{118}-b-PLA_{39} block copolymers in the aqueous solution tuned by PBS (ten times). PNIPAM exhibits a lower critical solution temperature (LCST) of ~32.5°C in the aqueous solution. This unique temperature-sensitive property of PNIPAM is widely investigated

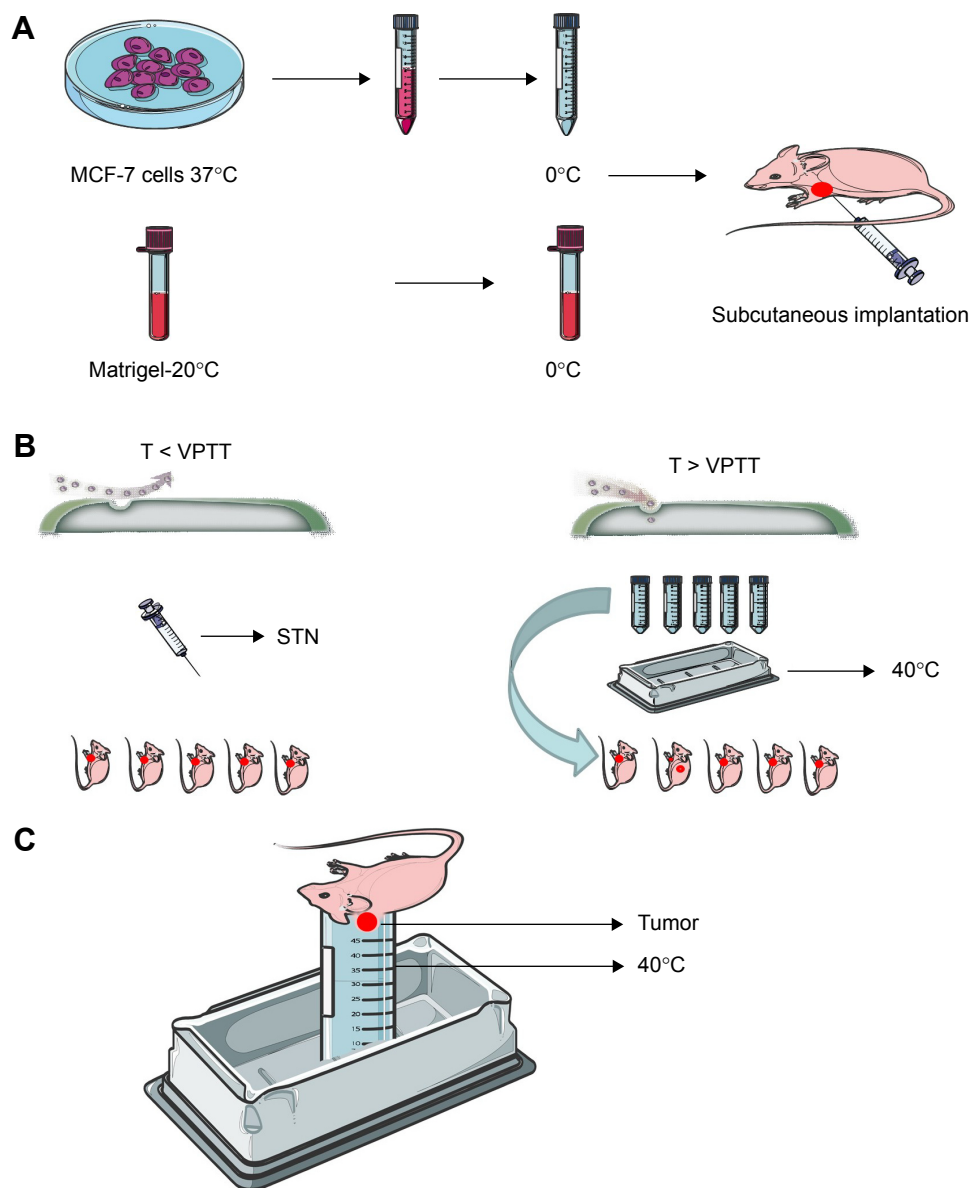**Figure 2** In vivo antitumor assays conducted by the in-house developed temperature tuner.
Notes: (**A**) The setting up of tumor model; (**B**) the comparison of antitumor assays between low and high temperature; and (**C**) the illustration of how to tune the tumor temperature. The left panel in (**B**) shows the experimental heating device for enhancing in vivo tumor temperature. This device was composed of 1 thermostatic water bath box and 5 test tubes (50 mL distilled water). When tumors had reached about 150 mm³, mice were administered with intravenous injection of STN. After 1 hour, the tumors on the mice of STN (40°C) group were immersed in the test tubes (50 mL distilled water in 40°C) for 10 minutes. The heating process was performed three times (10-minute interval) by five manipulators dependently.
Abbreviations: STN, shikonin-loaded thermosensitive nanomicelle; VPTT, volume phase transition temperature.

and has been suggested to hinge on a critical hydrophilic/hydrophobic balance between the chemical groups on the polymer. Referring to its different application, LCST can be tuned to larger or smaller than 32.5°C by hydrophilic or hydrophobic modification. As another hydrophilic monomer, DMAAm was successfully introduced to the PNIPAM chain backbone. The phase transition temperature of PID_{118}-b-PLA_{39} increased to ~39°C. The drug loading level of PID_{118}-b-PLA_{39} was 203 μg/mL.

The in vitro drug releasing profile of STN is shown in Figure 4B. The result showed that the shikonin release at physiological conditions (T =37°C) was very slow. Just half of the entrapped shikonin was released out within ~2 days. When the drug release was simulated in 40°C, the drug release rate was obviously enhanced, ~90% shikonin was released out within 10 hours without little difference in the release rate. Figure 4C shows the CMC value of PID_{118}-b-PLA_{39} in the aqueous solutions. As detailed in the previous publications,[31,32] the fluoroscopic method can be used to estimate hydrophobic microenvironments within micelles in the aqueous medium using pyrene as a hydrophobic fluorescent probe. At low concentration of the diblock copolymer, a shift of the excitation
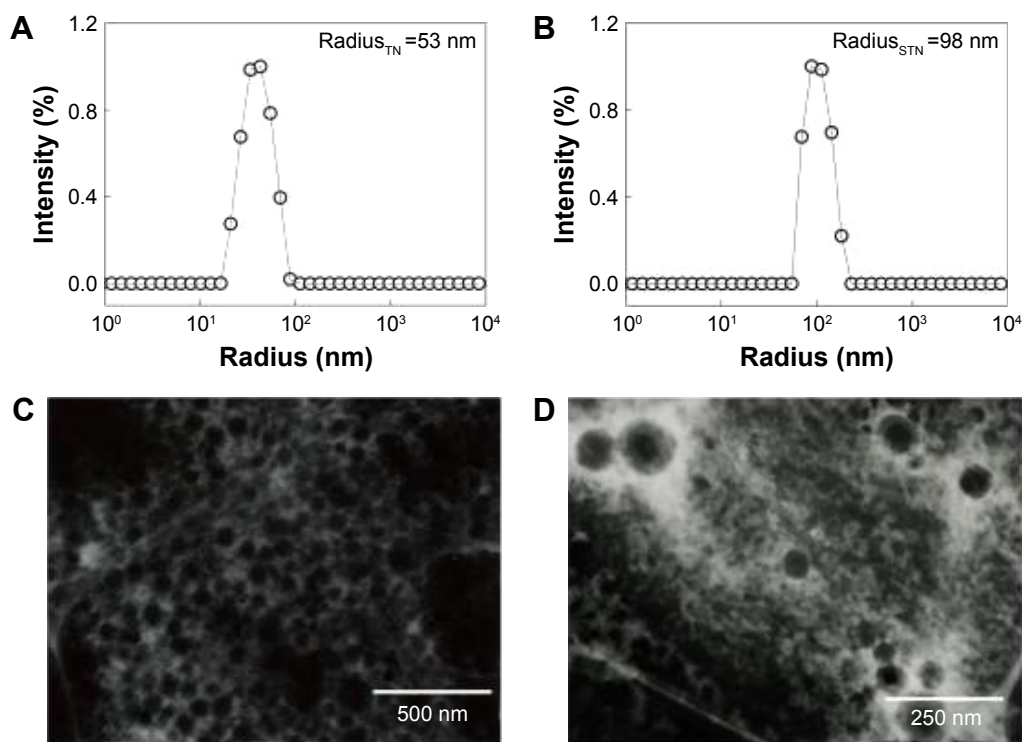
Figure 3 Characterization of TN and STN. The hydrodynamic diameter and the size distribution of TN (**A**) and STN (**B**) obtained in aqueous solution. The TEM morphology of such core-shell structural particles (**C** and **D**).
Abbreviations: TN, thermosensitive nanomicelle; STN, shikonin-loaded thermosensitive nanomicelle; TEM, transmission electron microscope.

band at 334 nm is negligible. As polymer concentration is increased, a red shift of the excitation band to 337 nm can be clearly detected. The intensity ratio I_{337}/I_{334} of the excitation spectrum changes as the logarithm of polymer concentration. Figure 4D shows the cytoxicity of PID_{118}-b-PLA_{39} micelles toward 293T cells incubated in a humidified condition at 37°C or 40°C with 5% CO_2. The viability of 293T cells has little change regardless of the polymer micelle concentration ranging from 3.91 to 1 mg/mL. These results indicate that the cytotoxicity of PID_{118}-b-PLA_{39} micelles is negligible. As shown in Figure 4E and F, the hydrodynamic diameter of bovine serum albumin (BSA), TN, and BSA-TN was dispersive distribution, which gave evidence of the good stability of TN in serum.

In vitro cellular internalization of TNs

Temperature-dependent intracellular uptake was further investigated by using flow cytometry and LSCM. As shown in Figure 5A, the temperature can regulate the cellular uptake of FTN through tuning the culture temperature. Figure 5B shows the time dependence of fluorescence intensity of free-FITC and FTN at the temperature of normal tissue at 37°C and 40°C. The green color was from FITC. At a given temperature of 37°C or 40°C, it was found that the intracellular fluorescence intensity at 40°C was much stronger than that obtained at 37°C.

In vitro cytotoxicity evaluation toward MCF-7 cells

The efficacy of the STN formulation to defeat cancer cells is evaluated by cytotoxicity assay. The concentration of micelles used for the cytotoxicity was larger than that of their CMC values (~1.84 and 3.98 mg/L). The cell surviving profile incubated with STN and FS at 37°C and 40°C was systemically investigated and compared. As shown in Figure 6A, the cytotoxicity difference between STN and FS was not so obvious at a given low shikonin concentration (<0.39 µg/mL). However, as the shikonin concentration in all formulations increased to 0.78 µg/mL, STN showed much higher toxicity than FS. In addition, the cytotoxicity profile could also be quantitatively evaluated by IC_{50}, which was defined as the drug concentration at which half the cells survived.[37,38] Figure 6B shows the IC_{50} profile of STN. It was found that the tumor-cell killing efficiency at 40°C was higher than that obtained at 37°C for STN. Figure 7 shows PCD of the MCF-7 cells, which shows a higher rate at 40°C.

In vivo tissue distribution of TNs

The tissue distribution of FTN was evaluated in mice bearing subcutaneous breast cancer. Figure 8 shows the distribution and tumor accumulation of free-FITC and FTN at 24 hours after injection. At 24 hours, there was a
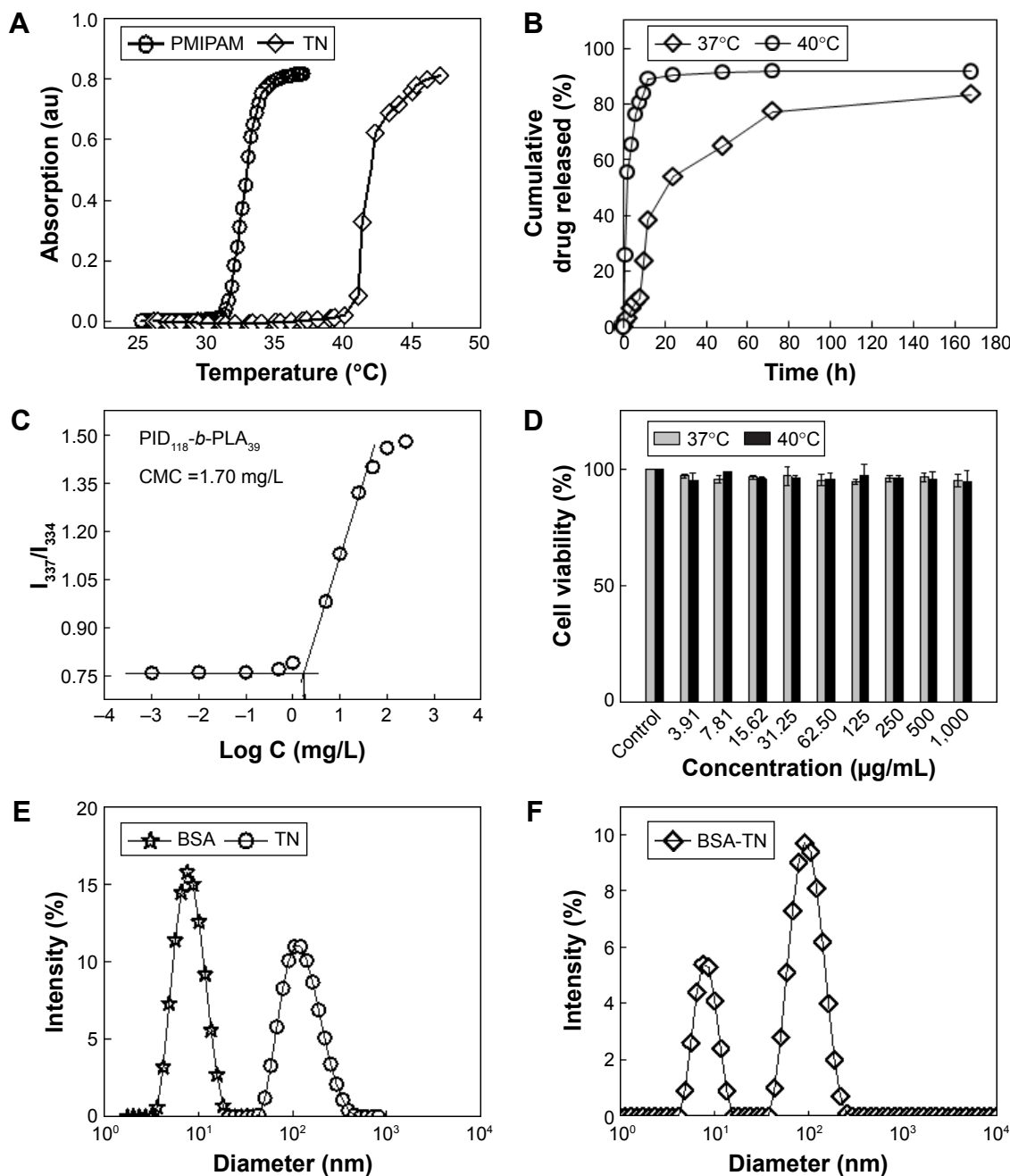
Figure 4 The physical chemistry properties of the TNs. (**A**) VPTT; (**B**) shikonin releasing profile; (**C**) CMC; (**D**) non-cytotoxicity profile of TNs; and (**E** and **F**) stability evaluation of TNs.
Abbreviations: TN, thermosensitive nanomicelle; VPTT, volume phase transition temperature; CMC, critical micelle concentration; PNIPAM, poly(N-isopropylacrymaide); PID, PNIPAM-c-DMAAm random copolymer; DMAAm, N,N-dimethylacrylamide; PLA, polylactic acid.

significant accumulation of FTN in the tumor, whereas little accumulation was observed for free-FITC. Compared with free-FITC, FTN exhibited superior targeting efficiency and accumulated in tumors. To clearly observe the fluorescence signals, the tumors and major organs were excised and collected at 24 hours after injection. The ex vivo fluorescent images of the excised tumors further demonstrated the higher accumulation of FTN compared with free-FITC. To investigate the binding and internalizing of the nanomicelles in vivo, the tumors and major organs were prepared into

pathological sections and were observed by the fluorescent microscope. The result showed that FITC accumulated profusely throughout the tumor tissues, which was consistent with the in vivo imaging data. In contrast, free-FITC showed only minimal accumulation.

In vivo antitumor efficiency evaluation

The therapeutic effect of STN was examined in mice bearing subcutaneous breast cancer. As mentioned above, the in vivo tumor accumulation of STNs was successfully realized by
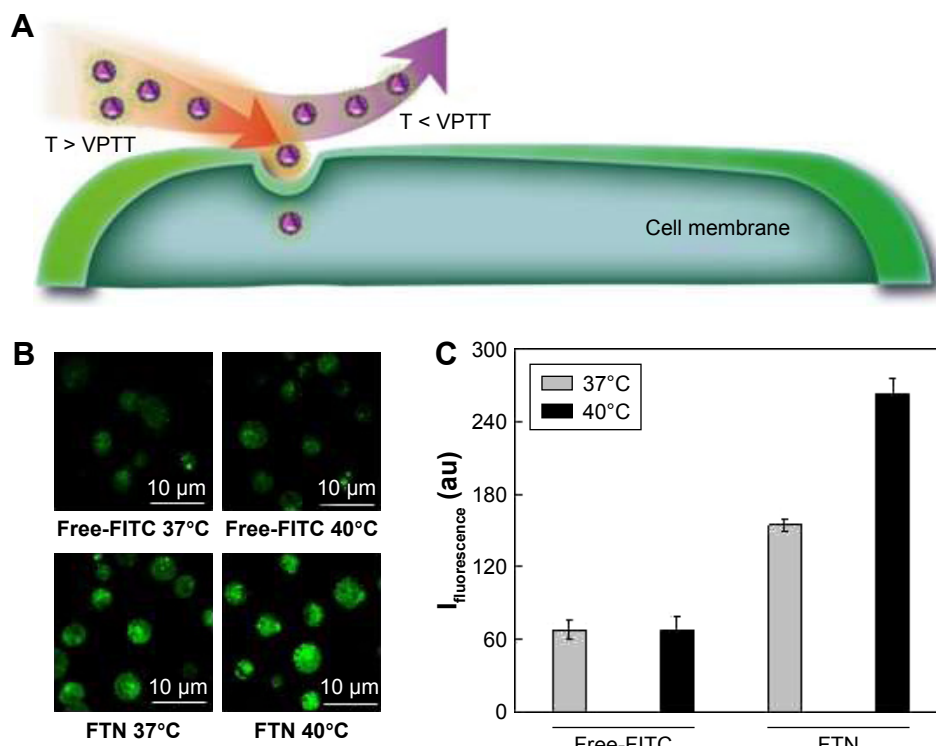
Figure 5 Cellular (MCF-7) uptake of free-FITC and FTN under LSCM and flow cytometry. The cellular mechanism of the uptake of micelle-loaded drug at different temperatures (**A**). MCF-7 cellular uptake of free-FITC and FTN under LSCM (**B**) and flow cytometry (**C**).
Note: 40°C was the temperature of cell incubator.
Abbreviations: FITC, fluorescein isothiocyanate; FTN, FITC-loaded thermosensitive nanomicelle; LSCM, confocal laser scanning microscope; VPTT, volume phase transition temperature; I, intensity.

the in-house developed heating device as shown in Figure 2. It should be noted that the micelles were injected into the mice bearing breast tumor firstly. After ~1 hour, the tumor was embedded in a 50 mL test tube, which was placed in

a water bath preheated to 40°C. The effects of temperature on the tumor suppression are illustrated in Figure 9A. At the end point at day 27 postinjection, the tumor volume of the STN (40°C) treatment group had resulted in a 74% decrease,
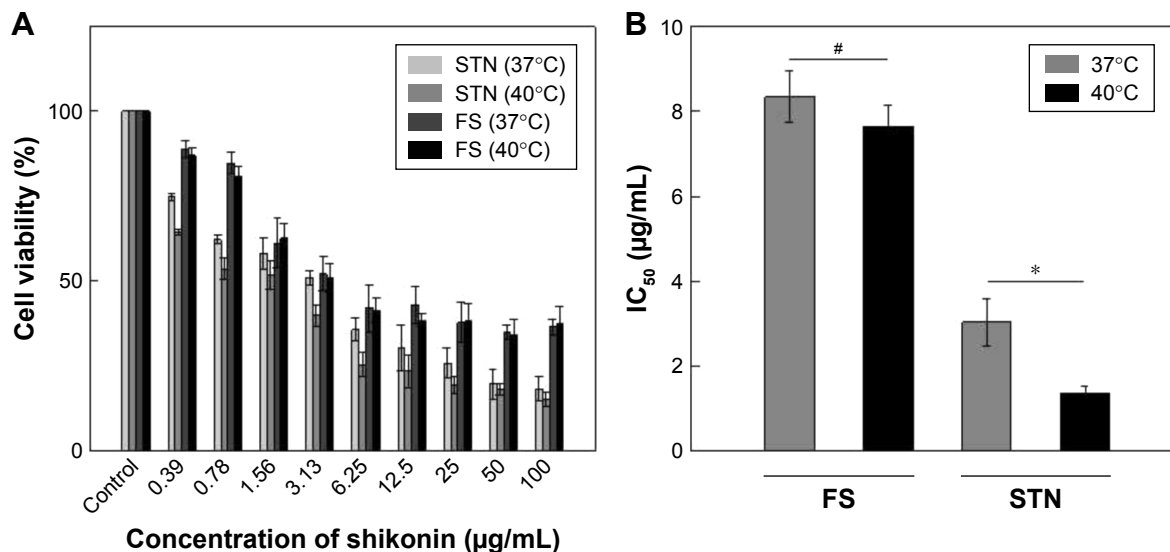

Figure 6 In vitro cytotoxicity of STN toward MCF-7 cells at 37°C and 40°C.
Notes: (**A**) The comparison of FS and STN cytotoxicity toward MCF-7 cells at 37°C and 40°C. (**B**) The comparison of FS and STN IC$_{50}$ toward MCF-7 cells at 37°C and 40°C. The higher temperature was tuned by increasing the incubator temperature. $P < 0.05$ was considered statistically significant. $*P < 0.05$; $\#P > 0.05$.
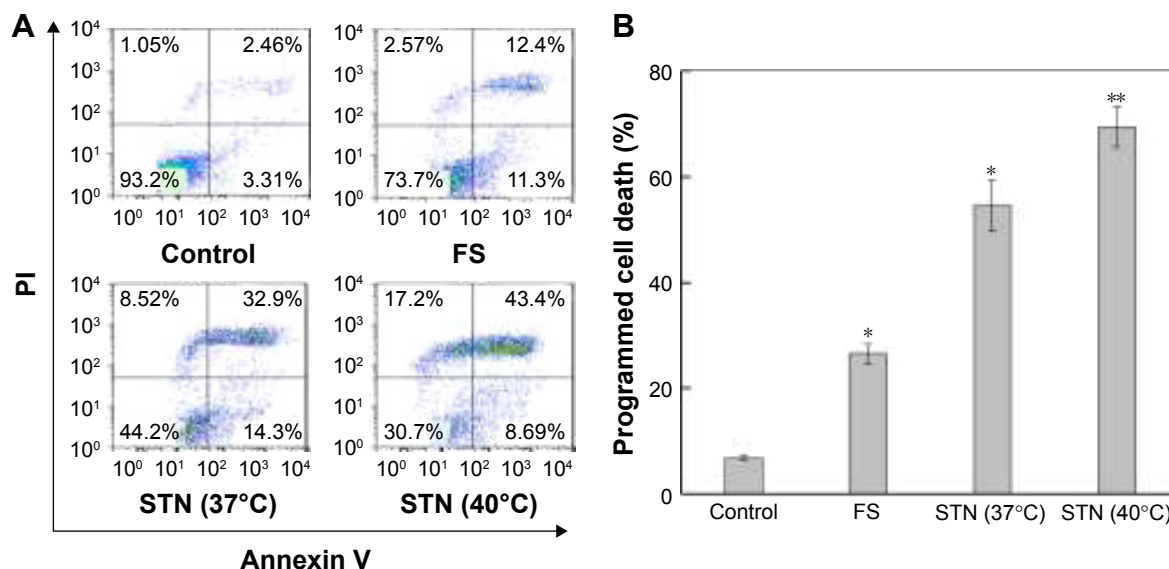**Abbreviations:** STN, shikonin-loaded thermosensitive nanomicelle; FS, free shikonin; IC$_{50}$, half maximal inhibitory concentration.

Figure 7 Annexin V/PI assay of STN toward MCF-7 cells at 37°C and 40°C.
Notes: (**A**) The annexin V/PI assay of Control, FS, STN (37°C) and STN (40°C) toward MCF-7 cells. (**B**) The comparison of the programmed cell death rates of control, FS, STN (37°C) and STN (40°C) toward MCF-7 cells. $P<0.05$ was considered statistically significant. $*P<0.05$; $**P<0.01$.
Abbreviations: PI, propidium iodide; STN, shikonin-loaded thermosensitive nanomicelle; FS, free shikonin.

whereas the tumor volume from the STN (37°C), FS, and PBS treatment groups had resulted in a 56%, 52%, and 23% decrease, respectively. By the end of the experiment, compared with the initial tumor volume (150 mm³), the tumor volume in the PBS-treated mice had increased by 22.1-fold, in the FS-treated mice had increased by 9.5-fold, and in the STN (40°C)-treated and STN (37°C)-treated mice had increased

only by 7.5-fold and 8.5-fold, respectively. The tumor volume of the STN (40°C)-treated group was significantly smaller than that of the other groups (PBS =3,859 mm³, FS =2,372 mm³, STN (37°C) =2,278 mm³, and STN (40°C) =1,235 mm³; STN (40°C) vs PBS: $P<0.001$, STN (40°C) vs FS: $P<0.001$, and STN (40°C) vs STN (37°C): $P<0.05$). The smaller tumor volume at 40°C indicated that

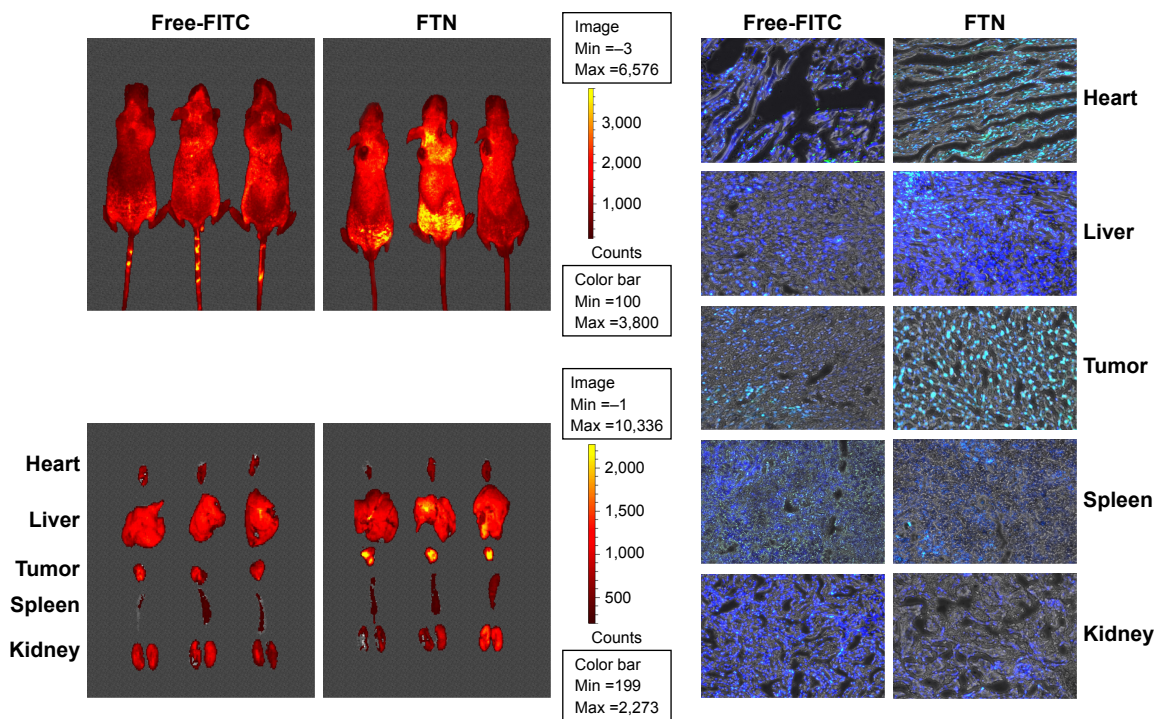**Figure 8** In vivo biodistribution of free-FITC and FTN in BALB/c nude mice bearing breast tumor at 37°C and 40°C.
Abbreviations: FITC, fluorescein isothiocyanate; FTN, FITC-loaded thermosensitive nanomicelle.
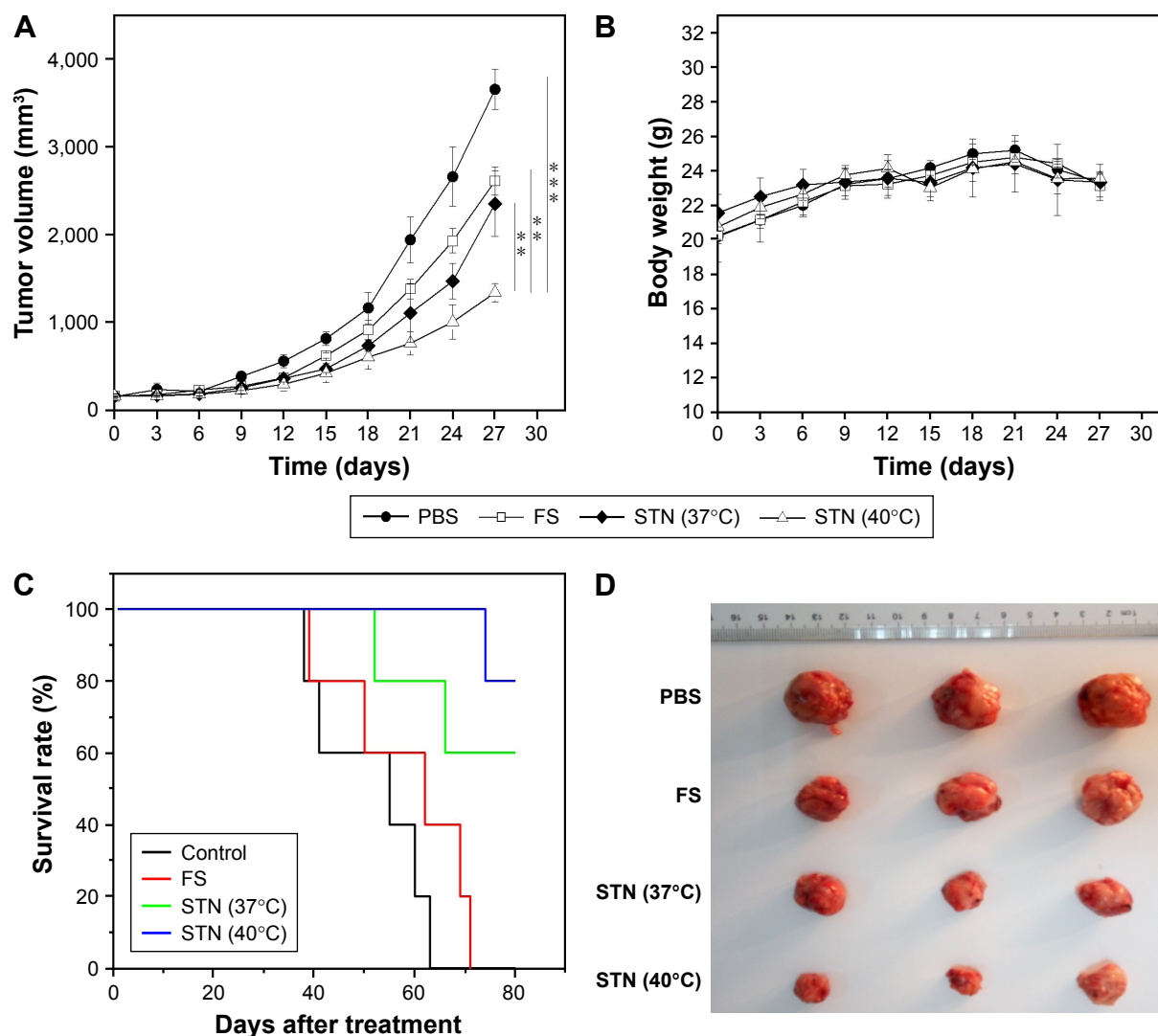
Figure 9 The inhibition of subcutaneous tumor growth by TN-loading shikonin in vivo at 37°C and 40°C. $P<0.05$ was considered statistically significant. $**P<0.01$; $***P<0.001$.
Note: (**A**) The time dependence of relative tumor volume. (**B**) The time dependence of body weight. (**C**) The survival rate of mice post treatment. (**D**) The damnation of solid tumor harvested from different groups.
Abbreviations: TN, thermosensitive nanomicelle; PBS, phosphate buffer solution; FS, free shikonin; STN, shikonin-loaded thermosensitive nanomicelle.

the in-house developed heating device for promoting in vivo tumor accumulation is successful. In addition, the toxicity of all treatments was measured by observing any behavioral changes after treatment and by monitoring mice weight. The results showed that all of the treatments were well tolerated by the mice bearing breast cancer tumors. None of the treated mice showed any noticeable behavioral change and any significant change in weight compared with the PBS control (Figure 9B), suggesting that FS and STN did not induce any noticeable behavioral change in mice and had no detrimental effect on the weight of mice.

Discussion

It is found that shikonin is an excellent candidate for cancer therapy, which can suppress tumor via its multi-targets with

mild toxicity to normal tissue. However, the therapeutic efficacy of shikonin is still limited due to its poor aqueous solubility, extensive first-pass metabolism, and low tumor accumulation. In this study, using the reversible deactivation radical polymerization (RAFT),[39,40] a micelle with thermosensitive shell and pH degradable core was developed for promoting the in vivo stabilization, cellular uptake, and cytotoxicity of shikonin. RAFT is applicable to a wide range of monomers under various experimental conditions.[41] By using this method, the thermosensitive copolymer PNIPAM-*co*-DMAAm was synthesized in benzene using HECPD as the RAFT agent and VA-086 as the initiator. This copolymer with OH termini (PID-OH) was used for linking another biodegradable hydrophobic block PLA via the ring-open polymerization (PID-*b*-PLA), resulting in the

block copolymer PID_{118}-b-PLA_{39}. Figure 1 shows the signal was not from hydrophobic PLA_{39} but from hydrophilic PID_{118}. The hydrophobic PLA_{39} was one well-defined core-shell structure according to the results of ^{1}H NMR. Both dynamic light scattering and TEM showed a narrow-size distribution (Figure 3), which plays a very important role in its in vivo stability and penetrating ability.[42,43]

VPTT of the PID_{118}-b-PLA_{39} block copolymer was ~39°C (Figure 4A). This VPTT value indicates that the PID_{118}-b-PLA_{39} micelles can safely encapsulate the anticancer drug and remain stable during blood circulation at the temperature of ~37°C. However, as the micelles arrive to the tumor site where the temperature is ~3°C–5°C higher than that of normal tissue, the PID shell will change from hydrophilic to hydrophobic resulting in high tumor accumulation. Additionally, as shown in Figure 4B, the shikonin release can also be enhanced as STN enter into the tumor at T > VPTT. Consequently, the solubility, cellular targeting, and intra-tumor release of shikonin are obviously enhanced by such STNs. It should be noted that CMC of the micelle plays an important role in micellar in vivo application, which was defined as the intersection of the lines drawn through the points of flat regions at low concentration and the drastically increasing regions at high concentration. The CMC value of the PID_{118}-b-PLA_{39} block copolymer is ~1.69 mg/L, which is relatively low for in vivo stability postinjection into the body and dilution with large volumes of surface-active components in blood.[44,45] It shows little changes regardless of the polymer micelle concentration ranging from 0.01 to 1 mg/mL both in 37°C and 40°C. These results indicate that the polymer cytotoxicity of PID_{118}-b-PLA_{39} micelles can be negligible, which is consistent with the results of previous studies.[28,46,47]

In the application, proteins in the blood may affect the micellar stability during their circulation. BSA was used to evaluate the effects of these serum proteins on micellar in vivo stability.[48–50] Figure 4E shows the size of BSA and micelle which was obtained. When BSA was mixed with the micelles, the distribution of BSA and micelle was not affected, which showed a little interaction between the nanoparticles' surface and BSA. This result gave evidence of the good stability of TN in serum. Thus, the application of PID_{118}-b-PLA_{39} for breast cancer therapy is very promising. According to the flow cytometric studies as shown in Figure 7, the cellular uptake of free-FITC is extremely lower than that of FTN at the same FITC concentration, which indicates that TN can obviously increase the dosage in tumor site. As shown in Figure 5A, FTN enhanced internalization into the cell at T > VPTT followed by an endosomal release.

But the free-FITC formulation was entrapped into the cell through a pathway of diffusion. So compared with the diffusion of FITC, the cellular uptake of the FTN formulation by the endocytosis process was much higher. In addition, the in vivo tissue distribution assay further demonstrated the increased penetrating efficacy of TN, which coincides with the in vivo tissue distribution as shown in Figure 8.

In addition, for the TN system, the cellular uptake at 40°C was much greater than that at 37°C, confirmed by LSCM as shown in Figure 5B. The green color was from FITC. In this study, VPTT was critical to increase the penetrating efficacy of FTN. The intracellular fluorescence intensity at 40°C was much stronger than that obtained at 37°C with a high fluorescent intensity (Figure 5C), which was attributed to T > VPTT. The results clearly indicate that the temperature can induce the micelles with thermosensitive shell system uptake. The mechanism should be related to the hydrophobic interaction between the micelles and cell membrane. Kumashiro et al previously reported that an ultrathin PNIPAM-grafted layer (<20 nm) on polystyrene surfaces successfully achieved temperature-modulated cell adhesion/detachment.[51] This is due to progressive dehydration and aggregation of the PNIPAM segments at the hydrophobic polystyrene interface with reduced molecular motion of covalently bound PNIPAM chains.[32,44] The thermosensitive PNIPAM shell can also be utilized to regulate the drug release as shown in Figure 4B.

In this study, STN (40°C) was readily internalized and released shikonin to the cytoplasm of breast cancer cells, resulting in an enhanced cytotoxic effect compared with STN (37°C) and FS. Although CCK-8 is measuring only an enzymatic activity, this suggests that STN (40°C) has a selective cytotoxic effect on breast cancer cells. The low number of cells surviving at 40°C clearly indicated that much more shikonin was transferred into the tumor cell. This was attributed to two factors: one was the improved shikonin release when the temperature increased (Figure 4B) and the other was the enhanced cellular uptake when the temperature increased above micellar VPTT (Figure 5). The results were consistent with the results of a previous study, which confirmed that TN could not only facilitate the penetrating efficacy of drug but also the internalization efficacy and cytotoxic effects on cancer cells.[28] It should be noted here that shikonin is an excellent drug for cancer cell inhibition through the complex mechanism including PCD. Shikonin can inhibit STAT(3), downregulate the expression of steroid sulfatase genes, inhibit EMT, and circumvent cancer drug resistance in breast cancer cells.[9–13] Figure 7 shows that PCD appeared

in the group treated by STNs. Compared with the control and FS group, PCD increased from 20% to 55%, which further increased to ~70% as T > VPTT. The results indicated that the cell death caused by STNs was attributed to two parts, one was suppressing the cancer cellular proliferation (Figure 6) and another was evoking the PCD. Here, both the necrosis and apoptosis might contribute to PCD. Moreover, both the

proliferation inhibition and PCD were obviously synergistically promoted by the STN's passive targeting function.

Although shikonin showed significant in vitro therapeutic efficacy through its multi-targets toward breast cancer, the efficiency was further promoted by STN's EPR and temperature-regulated passive targeting. As mentioned above, the in vivo conditions are very complex.
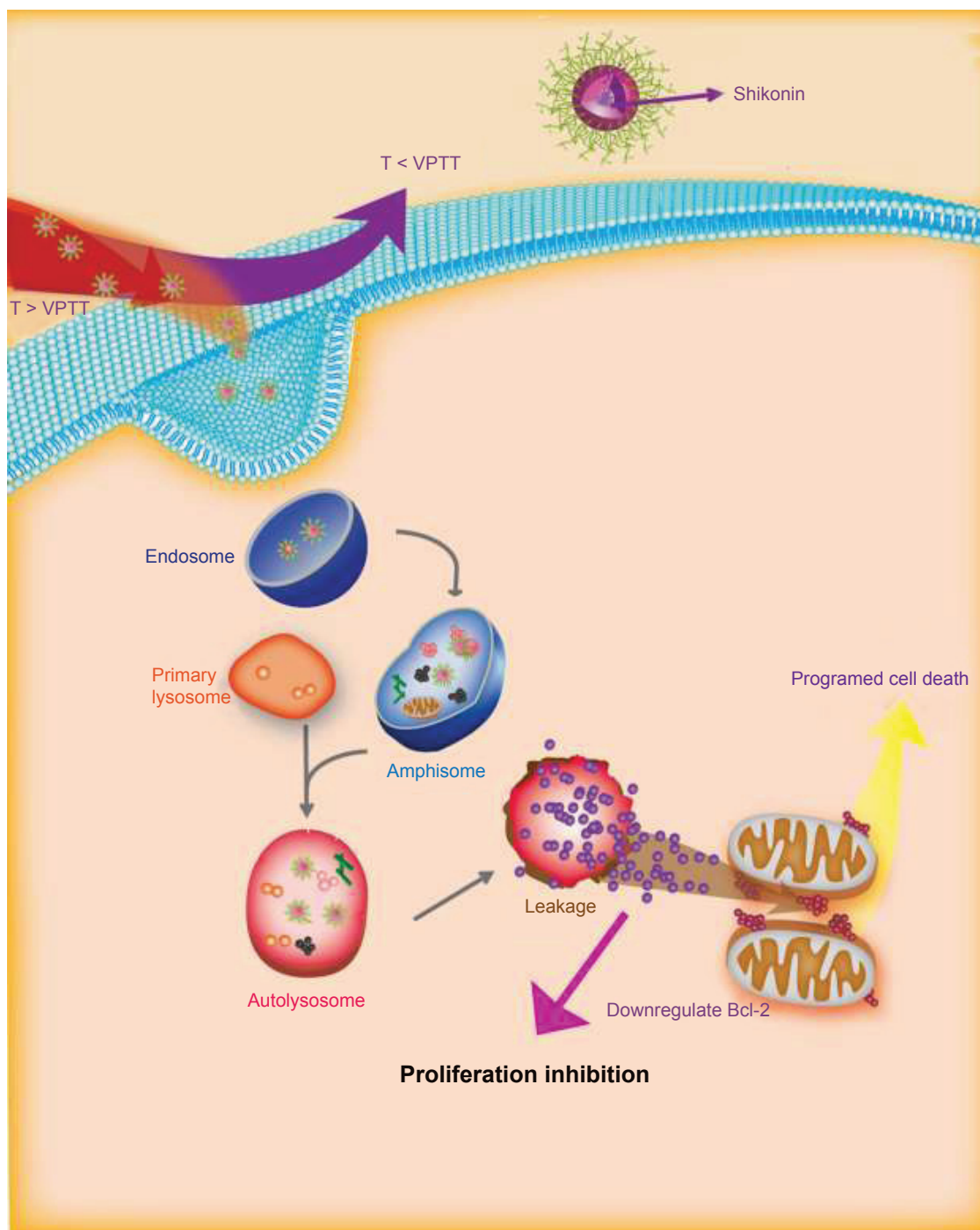

Figure 10 Illustration of the working mechanism of STN from intercellular to intracellular level.
Abbreviations: STN, shikonin-loaded thermosensitive nanomicelle; VPTT, volume phase transition temperature.

Demonstrating this issue is still a big challenge for the in vivo application of such thermosensitive STNs. The in vitro results offered us new hope that VPTT was expected to increase the in vivo penetrating efficacy. The critical point was increasing the in vivo tumor temperature. Thus, we conducted it for further demonstration. The water bath was used to increase the tumor temperature post the intravenous injection of STN, which ensured that the tumor temperature was higher than the temperature of normal tissue. The experimental details are shown in Figure 2. To the authors' knowledge, no similar efforts have been reported in previous literature. The tissue distribution and corresponding frozen sections clearly showed that the in vivo tumor accumulation of STNs could be enhanced by the special in vivo experimental device (Figure 8). Based on the successful biodistribution experiments, the in vivo therapeutic efficacy of STNs was further conducted as shown in Figure 9. Compared with the control (PBS and FS), the tumor volume of STN group was much smaller. Moreover, the tumor volume at 40°C was much smaller than that at 37°C due to the temperature-regulated passive targeting, which further indicated that the in vivo application of STNs could be realized by the experimental design used in this study (Figure 2).

Both the in vitro and in vivo antitumor efficiency demonstrated that the thermosensitive STNs formulation is high potent in cancer therapy. TNs not only help shikonin deliver to tumor vasculature in soluble formulation but also help penetrate extravascular tumor parenchyma and tumor cells. STN was internalized into the cell by endocytosis firstly, which was enhanced by the temperature-enhanced targeting followed by an endosomal release. The detailed cellular-level mechanism is illustrated in Figure 9. All the results obtained in this study have helped in elucidating the therapeutic efficacy of STN toward breast cancer. First, STN helped overcome the low aqueous solubility of shikonin, which is the major barrier to its oral and internal administration. Moreover, STN can obviously accumulate in breast cancer tumors due to the EPR effect and its thermosensitive passive targeting activity promoted by the in-house developed experimental device (Figure 10). Later, STN was first internalized into the cell by endocytosis followed by an endosomal release. Second, STN can obviously suppress the breast cancer cells via its multi-targets. The detailed mechanism of the death will be further disclosed in future studies. Third, the cellular death can be obviously enhanced by the passive targeting of TN as $T > $ VPTT, which indicates that such STNs are a potential candidate for cancer therapy.

Conclusion

In order to improve the tumor accumulation and solubility of the Chinese traditional medicine shikonin, the RAFT polymerization was used to prepare one thermosensitive biodegradable block copolymer PID_{118}-b-PLA_{39} with symmetric hydrophobic blocks. In addition, the in-house developed experimental device was used to improve the in vivo tumor accumulation of micelles, which targets the high temperature (~40°C) of tumor tissue. The physical chemistry properties of the corresponding well-defined core-shell structural micelles were systemically investigated. TN helped overcome the low aqueous solubility of shikonin, which is the major barrier to its oral and internal administration. Compared with the normal physiological conditions (T =37°C), the shikonin release and the hydrophobic core degradation were obviously enhanced under the simulated tumor tissue condition (T =40°C). In addition, it was found that the intracellular uptake was obviously enhanced (four times) above the micellar VPTT. Thus, the mechanism between intelligent property and therapeutic effect was clarified by comparing their cytotoxicity against breast cancer at 37°C and 40°C in vitro and in vivo. All this confirmed that the thermosensitive biodegradable micelles are a promising carrier of shikonin for breast cancer therapy.

Disclosure

The authors report no conflicts of interest in this work.

References

1. Siegel RL, Miller KD, Jemal A. Cancer statistics, 2016. *CA Cancer J Clin*. 2016;66(1):7–30.
2. Miller KD, Siegel RL, Lin CC, et al. Cancer treatment and survivorship statistics, 2016. *CA Cancer J Clin*. 2016;66(4):271–289.
3. Andre F, Slimane K, Bachelot T, et al. Breast cancer with synchronous metastases: trends in survival during a 14-year period. *J Clin Oncol*. 2004;22(16):3302–3308.
4. Dawood S, Broglio K, Gonzalez-Angulo AM, Buzdar AU, Hortobagyi GN, Giordano SH. Trends in survival over the past two decades among white and black patients with newly diagnosed stage IV breast cancer. *J Clin Oncol*. 2008;26(30):4891–4898.
5. Cardoso F, Beishon M, Cardoso MJ, et al. Global status of advanced/metastatic breast cancer (ABC/mBC): A Decade Report 2005–2015. *Eur J Cancer*. 2016;57:S5–S6.

6. Li W, Zhao H, Qian W, et al. Chemotherapy for gastric cancer by finely tailoring anti-Her2 anchored dual targeting immunomicelles. *Biomaterials*. 2012;33(21):5349–5362.

7. Kim MG, Shon Y, Kim J, Oh YK. Selective activation of anticancer chemotherapy by cancer-associated fibroblasts in the tumor microenvironment. *J Natl Cancer Inst*. 2016;109(1). pii: djw186.

8. Couladouros EA, Strongilos AT, Papageorgiou VP, Plyta ZF. A new efficient route for multigram asymmetric synthesis of alkannin and shikonin. *Chemistry*. 2002;8(8):1795–1803.

9. Hou Y, Guo T, Wu C, He X, Zhao M. Effect of shikonin on human breast cancer cells proliferation and apoptosis in vitro. *Yakugaku Zasshi*. 2006;126(12):1383–1386.

10. Thakur R, Trivedi R, Rastogi N, Singh M, Mishra DP. Inhibition of STAT3, FAK and Src mediated signaling reduces cancer stem cell load, tumorigenic potential and metastasis in breast cancer. *Sci Rep*. 2015;5:10194.

11. Zhang Y, Qian RQ, Li PP. Shikonin, an ingredient of Lithospermum erythrorhizon, down-regulates the expression of steroid sulfatase genes in breast cancer cells. *Cancer Lett*. 2009;284(1):47–54.

12. Hong D, Jang SY, Jang EH, et al. Shikonin as an inhibitor of the LPS-induced epithelial-to-mesenchymal transition in human breast cancer cells. *Int J Mol Med*. 2015;36(6):1601–1606.

13. Jang SY, Lee JK, Jang EH, Jeong SY, Kim JH. Shikonin blocks migration and invasion of human breast cancer cells through inhibition of matrix metalloproteinase-9 activation. *Oncol Rep*. 2014;31(6):2827–2833.

14. Wu H, Xie J, Pan Q, Wang B, Hu D, Hu X. Anticancer agent shikonin is an incompetent inducer of cancer drug resistance. *PLoS One*. 2013; 8(1):e52706.

15. Assimopoulou AN, Papageorgiou VP. Encapsulation of isohexenyl-naphthazarins in cyclodextrins. *Biomed Chromatogr*. 2004;18(4): 240–247.

16. Albreht A, Vovk I, Simonovska B. Addition of beta-lactoglobulin produces water-soluble shikonin. *J Agric Food Chem*. 2012;60(43): 10834–10843.

17. Li W, Feng SS, Guo Y. Block copolymer micelles for nanomedicine. *Nanomedicine*. 2012;7(2):169–172.

18. Li W, Wei H, Li H, Gao J, Feng SS, Guo Y. Cancer nanoimmunotherapy using advanced pharmaceutical nanotechnology. *Nanomedicine*. 2014; 9:2587–2605.

19. Lee RS, Lin CH, Aljuffali IA, Hu KY, Fang JY. Passive targeting of thermosensitive diblock copolymer micelles to the lungs: synthesis and characterization of poly(N-isopropylacrylamide)-block-poly (ε-caprolactone). *J Nanobiotechnology*. 2015;13:42.

20. Deng H, Zhang Y, Wang X, et al. Balancing the stability and drug release of polymer micelles by the coordination of dual-sensitive cleavable bonds in cross-linked core. *Acta Biomater*. 2015;11(1): 126–136.

21. Wei F, Yingzhe W, Xin D, Lei S, DeAngelo M, Chalet T. Reduction-responsive crosslinked micellar nanoassemblies for tumor-targeted drug delivery. *Pharm Res*. 2015;32(4):1325–1340.

22. Saiz LM, Oyanguren PA, Galante MJ, Zucchi IA. Light responsive thin films of micelles of PS-b-PVP complexed with diazophenol chromophore. *Nanotechnology*. 2014;25(6):065601.

23. Deng L, Ren J, Li J, et al. Magnetothermally responsive star-block copolymeric micelles for controlled drug delivery and enhanced thermo-chemotherapy. *Nanoscale*. 2015;7(21):9655–9663.

24. Ji G, Yang J, Chen J. Preparation of novel curcumin-loaded multifunctional nanodroplets for combining ultrasonic development and targeted chemotherapy. *Int J Pharm*. 2014;466(1–2):314–320.

25. Chen CY, Kim TH, Wu WC, et al. pH-dependent, thermosensitive polymeric nanocarriers for drug delivery to solid tumors. *Biomaterials*. 2013;34(18):4501–4509.

26. Li G, Liu J, Pang Y, et al. Polymeric micelles with water-insoluble drug as hydrophobic moiety for drug delivery. *Biomacromolecules*. 2011; 12(6):2016–2026.

27. Theerasilp M, Nasongkla N. Comparative studies of poly(ε-caprolactone) and poly(D,L-lactide) as core materials of polymeric micelles. *J Microencapsul*. 2013;30(4):390–397.

28. Li W, Li JF, Gao J, et al. The fine-tuning of thermosensitive and degradable polymer micelles for enhancing intracellular uptake and drug release in tumors. *Biomaterials*. 2011;32(15):3832–3844.

29. Li W, Guo Q, Zhao H, et al. Novel dual-control poly(N-isopropylacrylamide-co-chlorophyllin) nanogels for improving drug release. *Nanomedicine (Lond)*. 2012;7(3):383–392.

30. Li W, Feng SS, Guo Y. Tailoring polymeric micelles to optimize delivery to solid tumors. *Nanomedicine (Lond)*. 2012;7(8):1235–1252.

31. Nakayama M, Okano T. Polymer terminal group effects on properties of thermoresponsive polymeric micelles with controlled outer-shell chain lengths. *Biomacromolecules*. 2005;6(4): 2320–2327.

32. Akimoto J, Nakayama M, Sakai K, Okano T. Molecular design of outermost surface functionalized thermoresponsive polymeric micelles with biodegradable cores. *J Polym Sci A Polym Chem*. 2008; 46(21):7127–7137.

33. Akimoto J, Nakayama M, Sakai K, Okano T. Thermally controlled intracellular uptake system of polymeric micelles possessing poly (N-isopropylacrylamide)-based outer coronas. *Mol Pharm*. 2010;7(4): 926–935.

34. Shogren R. Water vapor permeability of biodegradable polymers. *J Polym Environ*. 1997;5(2):91–95.

35. Vyhnalkova R, Eisenberg A, van de Ven TG. Loading and release mechanisms of a biocide in polystyrene-block-poly(acrylic acid) block copolymer micelles. *J Phys Chem B*. 2008;112(29):8477–8485.

36. Kabanov AV, Nazarova IR, Astafieva IV, et al. Micelle formation and solubilization of fluorescent probes in poly(oxyethylene-b-oxypropylene-b-oxyethylene) solutions. *Macromolecules*. 1995;28(7):2303–2314.

37. Seow WY, Xue JM, Yang YY. Targeted and intracellular delivery of paclitaxel using multi-functional polymeric micelles. *Biomaterials*. 2007;28(9):1730–1740.

38. Sun B, Ranganathan B, Feng SS. Multifunctional poly(D,L-lactide-co-glycolide)/montmorillonite (PLGA/MMT) nanoparticles decorated by Trastuzumab for targeted chemotherapy of breast cancer. *Biomaterials*. 2008;29(4):475–486.

39. Nai YH, Jones RC, Breadmore MC. Sieving polymer synthesis by reversible addition fragmentation chain transfer polymerization. *Electrophoresis*. 2013;34(22–23):3189–3197.

40. Moad G, Chong YK, Postma A, Rizzardo E, Thang SH. Advances in RAFT polymerization: the synthesis of polymers with defined end-groups. *Polymer*. 2005;46(19):8458–8468.

41. Zhu X, Sun Y, Chen D, et al, Mastocarcinoma therapy synergistically promoted by lysosome dependent apoptosis specifically evoked by 5-Fu@nanogel system with passive targeting and pH activatable dual function. *J Control Release*. 2017; 254:107–118.

42. Kataoka K, Matsumoto T, Yokoyama M, et al. Doxorubicin-loaded poly(ethylene glycol)-poly(beta-benzyl-L-aspartate) copolymer micelles: their pharmaceutical characteristics and biological significance. *J Control Release*. 2000;64(1–3):143–153.

43. Itoh T, Abe I, Tamamitsu T, Shimomoto H, Inoue K, Ihara E. Surface structure of stimuli-responsive polystyrene particles prepared by dispersion polymerization with a polystyrene/poly(L-lysine) block copolymer as a stabilizer. *Polymer*. 2014;55(16):3961–3969.

44. Nakayama M, Chung JE, Miyazaki T, Yokoyama M, Sakai K, Okano T. Thermal modulation of intracellular drug distribution using thermo-responsive polymeric micelles. *React Funct Polym*. 2007;67(11): 1398–1407.

45. Yokoyama M, Okano T, Sakurai Y, Ekimoto H, Shibazaki C, Kataoka K. Toxicity and antitumor activity against solid tumors of micelle-forming polymeric anticancer drug and its extremely long circulation in blood. *Cancer Res*. 1991;51(12):3229–3236.

46. Ehmann F, Sakai-Kato K, Duncan R, et al. Next-generation nanomedicines and nanosimilars: EU regulators' initiatives relating to the development and evaluation of nanomedicines. *Nanomedicine (Lond)*. 2013;8(5):849–856.

47. Nyström AM, Fadeel B. Safety assessment of nanomaterials: implications for nanomedicine. *J Control Release*. 2012;161(2):403–408.

48. Laville M, Babin J, Londono I, et al. Polysaccharide-covered nanoparticles with improved shell stability using click-chemistry strategies. *Carbohydr Polym*. 2013;93(2):537–546.

49. Katas H, Raja MA, Lam KL. Development of chitosan nanoparticles as a stable drug delivery system for protein/siRNA. *Int J Biomater*. 2013; 2013(4):146320.

50. Petersen LK, Sackett CK, Narasimhan B. High-throughput analysis of protein stability in polyanhydride nanoparticles. *Acta Biomater*. 2010; 6(10):3873–3881.

51. Kumashiro Y, Yamato M, Okano T. Cell attachment-detachment control on temperature-responsive thin surfaces for novel tissue engineering. *Ann Biomed Eng*. 2010;38(6):1977–1988.